nature medicine

Lrp5 functions in bone to regulate bone mass

Yajun Cui[1,2], Paul J Niziolek[3–5], Bryan T MacDonald[6,7], Cassandra R Zylstra[8], Natalia Alenina[9], Daniel R Robinson[8], Zhendong Zhong[8], Susann Matthes[9], Christina M Jacobsen[1], Ronald A Conlon[2], Robert Brommage[10], Qingyun Liu[10], Faika Mseeh[10], David R Powell[10], Qi M Yang[10], Brian Zambrowicz[10], Han Gerrits[11], Jan A Gossen[11], Xi He[6,7], Michael Bader[9], Bart O Williams[8], Matthew L Warman[1,12,13] & Alexander G Robling[4,5]

The human skeleton is affected by mutations in low-density lipoprotein receptor-related protein 5 (LRP5). To understand how LRP5 influences bone properties, we generated mice with osteocyte-specific expression of inducible *Lrp5* mutations that cause high and low bone mass phenotypes in humans. We found that bone properties in these mice were comparable to bone properties in mice with inherited mutations. We also induced an *Lrp5* mutation in cells that form the appendicular skeleton but not in cells that form the axial skeleton; we observed that bone properties were altered in the limb but not in the spine. These data indicate that Lrp5 signaling functions locally, and they suggest that increasing LRP5 signaling in mature bone cells may be a strategy for treating human disorders associated with low bone mass, such as osteoporosis.

The skeleton is influenced by environmental, genetic, neurologic, endocrine, paracrine and autocrine factors. Efforts to identify pathways that affect bone health have been facilitated by genetic studies in individuals with abnormally low or abnormally high bone mass[1–6]. A key role for LRP5 was identified using these approaches. Individuals with osteoporosis-pseudoglioma syndrome, a disorder involving low bone mass, have loss-of-function mutations in *LRP5* (refs. 1,7), whereas heterozygous missense mutations in *LRP5* have been observed in individuals with dominantly inherited high bone mass (HBM)[2,3,8].

The mechanism by which LRP5 regulates bone mass has not been fully delineated. Studies in several laboratories indicate that LRP5 can function as a co-receptor in the canonical Wnt signaling cascade *in vivo* and *ex vivo*[1,3,9–12]. Furthermore, mice with genetic alterations in other components of the canonical Wnt signaling pathway have been shown to have alterations in bone mass; this is consistent with this pathway's importance in bone mass accrual[10,13–16]. A direct role for LRP5 in osteoblast-lineage cells has been proposed based on studies in mice that overexpress *LRP5* cDNAs driven by a rat type-1 collagen promoter[17]. However, phenotypes resulting from transgene-driven overexpression of a protein may not accurately reflect the endogenous protein's function.

We generated two lines of *Lrp5* knock-in mice (see **Supplementary Methods**), each containing a missense mutation found in human HBM. Both missense mutant proteins had been shown to be comparable to wild-type human LRP5 in their ability to transduce canonical Wnt signaling in transfected cells[9]. However, the mutants differed in their efficiency of trafficking to the cell surface, as well as in their interactions with the chaperone protein MESD and the extracellular inhibitors Dickkopf homolog 1 (DKK1) and sclerostin (SOST)[9,11,18]. We designed the *Lrp5* knock-in alleles to function as HBM-causing alleles after Cre recombinase (Cre)-mediated recombination. This enabled us to compare the effect of inheriting an *Lrp5* HBM allele, such that the allele is present in all cells, with the effect of activating an *Lrp5* HBM allele in a cell type–specific or tissue-specific manner. We also generated mice with floxed wild-type (WT) *Lrp5* alleles that could be converted to knockout alleles after Cre-mediated recombination. This enabled us to compare the effect of inheriting inactive *Lrp5* with the effect of inactivating *Lrp5* in a cell type–specific or tissue-specific manner.

RESULTS

Inherited *Lrp5* HBM alleles increase bone mass

Exon 3 of mouse *Lrp5* encodes the residues we mutated to HBM-causing alleles (p.G171V and p.A214V). Our targeting vector incorporated a neomycin-resistance cassette (Neo^R) flanked by *loxP* sites (**Fig. 1a**). Because Neo^R is driven by a strong promoter and transcribed in the opposite direction of *Lrp5*, we anticipated that Neo^R would interfere with *Lrp5* transcription and thereby cause *Lrp5* Neo^R-containing HBM alleles (G_N and A_N) to be poorly expressed. Mice with the *Lrp5* genotypes G_N/G_N or A_N/A_N had reduced expression compared to WT mice (**Fig. 1b**). Cre-mediated excision of Neo^R (G and A) enhanced expression such that mice with genotypes G/G or

[1]Orthopedic Research Laboratories, Department of Orthopedic Surgery, Children's Hospital, Boston, Massachusetts, USA. [2]Department of Genetics, Case Western Reserve University School of Medicine, Cleveland, Ohio, USA. [3]Weldon School of Biomedical Engineering, Purdue University, West Lafayette, Indiana, USA. [4]Department of Anatomy & Cell Biology, Indiana University School of Medicine, Indianapolis, Indiana, USA. [5]Department of Biomedical Engineering, Indiana University School of Medicine, Indianapolis, Indiana, USA. [6]F.M. Kirby Neurobiology Center, Children's Hospital, Boston, Massachusetts, USA. [7]Department of Neurology, Harvard Medical School, Boston, Massachusetts, USA. [8]Center for Skeletal Disease Research, Van Andel Research Institute, Grand Rapids, Michigan, USA. [9]Max Delbrück Center for Molecular Medicine, Berlin-Buch, Germany. [10]Lexicon Pharmaceuticals, The Woodlands, Texas, USA. [11]Merck Sharp & Dohme Research Laboratories, Oss, The Netherlands. [12]Howard Hughes Medical Institute, Children's Hospital, Boston, Massachusetts, USA. [13]Department of Genetics, Harvard Medical School, Boston, Massachusetts, USA. Correspondence should be addressed to M.L.W. (matthew.warman@childrens.harvard.edu).

Received 14 December 2010; accepted 27 April 2011; published online 22 May 2011; doi:10.1038/nm.2388

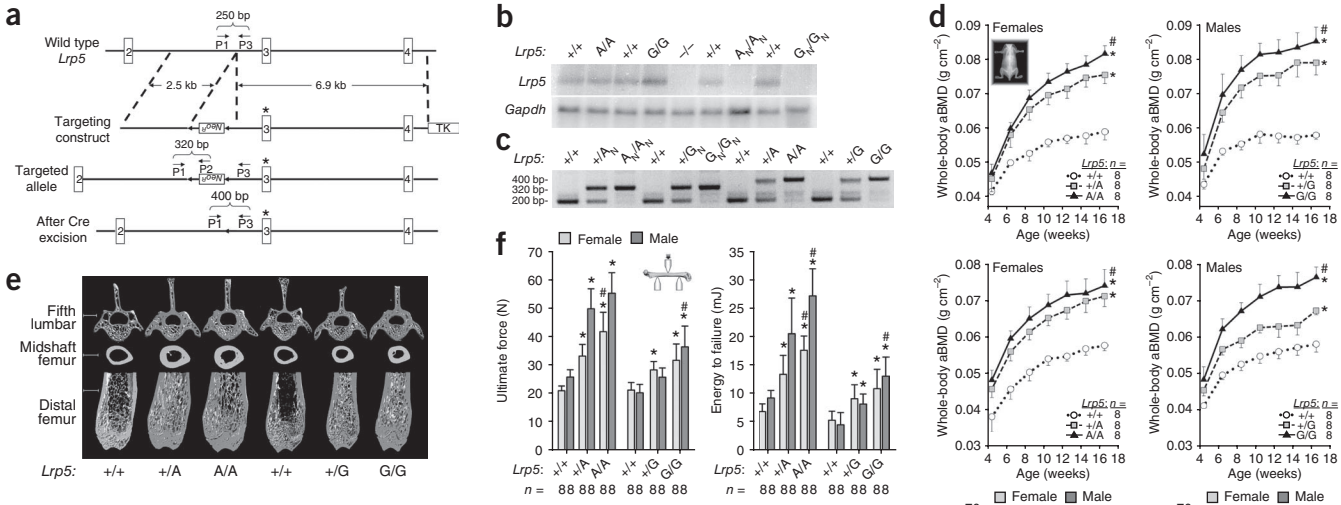

Lrp5:	+/+ (n = 4)	A/A (n = 4)	G/G (n = 4)
BFR/BS ($\mu m^3\ \mu m^{-2}\ yr^{-1}$)	125.5 ± 7.8	415.2 ± 35.1*	335.8 ± 19.3*
MAR ($\mu m\ d^{-1}$)	1.15 ± 0.14	2.46 ± 0.22*	2.04 ± 0.14*
MS/BS (%)	31.5 ± 2.2	46.2 ± 1.7*	45.2 ± 1.7*

Figure 1 Generation and characterization of HBM-causing *Lrp5* knock-in mice. (**a**) Schematic depicting the targeting and genotyping strategies for *Lrp5* HBM alleles. The 5′ targeting arm contains a neomycin-resistance cassette (*Neo*^{R}) flanked by *loxP* sites (arrowheads). The 3′ targeting arm begins in intron 2 and extends into intron 4, and is followed by a thymidine kinase (TK) cassette. Site-directed mutagenesis altered specific amino acid residues encoded by *Lrp5* exon 3 (asterisks). The relative locations and orientation of primers used for PCR genotyping and their expected amplimer sizes are noted. (**b**) Autoradiographs of a northern blot containing whole-bone total RNA from mice with different *Lrp5* genotypes initially hybridized with a radioactive *Lrp5* cDNA probe (top) and subsequently with a glyceraldehyde 3-phosphate dehydrogenase (*Gapdh*) cDNA probe which serves as a loading control (bottom). (**c**) Photograph of an agarose gel containing PCR amplimers derived from genomic DNA of mice with different *Lrp5* genotypes. (**d**) Graphs depicting the areal bone mineral density (aBMD) measured by dual-energy X-ray absorptiometry (DEXA) in mice with different *Lrp5* genotypes; mice followed until the age of 16.5 weeks (top and middle). Graphs depicting the percentage of trabecular bone volume in the total volume (BV/TV) of the distal femora and fifth lumbar vertebrae of 16.5-week-old male and female mice with different *Lrp5* genotypes (bottom). (**e**) Representative μCT scan images obtained from 16.5-week-old mice with different *Lrp5* genotypes. Scale bars, 1 mm. (**f**) Graphs depicting biomechanical properties of whole femora in a three-point bending assay from 16.5-week-old mice with different *Lrp5* genotypes. (**g**) Representative images of new bone formation assessed by double calcein labeling of mice with different *Lrp5* genotypes. Bone formation rates/bone surface area (BFR/BS); mineral apposition rates (MAR); mineralizing surface/bone surface (MS/BS). The numbers of mice studied are indicated. Error bars show means ± s.d. *$P < 0.05$ versus WT mice; #$P < 0.05$ versus heterozygous *Lrp5* HBM mice.

A/A had expression that was comparable to WT expression (**Fig. 1b**). We designed a PCR assay to distinguish *Lrp5* WT, *Neo*^{R}-containing (G_N or A_N), and *Neo*^{R}-excised HBM (G or A) alleles (**Fig. 1c**).

After creating conditional alleles that can be converted to HBM-causing alleles by Cre, we investigated whether mice with inherited *Lrp5* HBM alleles (*Neo*^{R}-excised) recapitulated the human HBM phenotype. Compared with WT mice, mice with *Lrp5* HBM alleles had increased bone mass (**Fig. 1d**,**e**, **Supplementary Fig. 1** and **Supplementary Table 1**), bone strength (**Fig. 1f**) and bone formation rates (**Fig. 1g**). When we intercrossed mice with *Lrp5* HBM alleles to *BAT-lacZ* transgenic mice (*BAT-lacZ* is a Wnt reporter mouse strain that expresses *lacZ* in response to canonical Wnt signaling[19]), we observed increased *lacZ* expression in cortical bone homogenates from the offspring that inherited *Lrp5* HBM alleles compared to offspring that inherited WT alleles; we also observed increased expression of *Axin2* (encoding axin-2), a known Wnt target gene[20], in mice with *Lrp5* HBM alleles compared to mice with WT alleles (**Supplementary Fig. 1**).

Lrp5 HBM expression in osteocytes increases bone mass

Mice heterozygous for alleles G_N or A_N (see **Supplementary Methods**) had bone mass comparable to WT mice (**Fig. 2a**, **Supplementary Figs. 2** and **3** and **Supplementary Table 2**), thereby indicating that decreased expression of the G_N or A_N allele was partially compensated for by its increased function. Because Cre converts alleles G_N and A_N to alleles G and A, respectively, we tested whether increasing *Lrp5* HBM allele expression in osteocytes would affect bone mass. We crossed mice with G/G_N or A/A_N genotypes to mice hemizygous for a transgene, *Dmp1-Cre*, in which a dentin matrix protein 1 (encoded by *Dmp1*) regulatory sequence drives Cre expression in osteocytes[21]. Offspring that inherited the *Lrp5* HBM allele (G or A) had high bone mass, independent of whether they inherited *Dmp1-Cre* (**Fig. 2b**,**c**). Offspring that inherited the *Lrp5 Neo*^{R}-containing allele (G_N or A_N), and not *Dmp1-Cre*, had normal bone mass (**Fig. 2b**,**c** and **Supplementary Figs. 3** and **4**). Offspring that inherited the *Lrp5 Neo*^{R}-containing allele (G_N or A_N) and *Dmp1-Cre* had increased bone mass (**Fig. 2b**,**c** and **Supplementary Figs. 3** and **4**), thus supporting a local role for Lrp5 signaling in bone. We confirmed that the *Dmp1-Cre* transgene was expressed in bone (**Fig. 2d**). Furthermore, conversion of alleles G_N and A_N to alleles G and A, respectively, in mouse osteocytes, had the same effect on bone as did inheriting G and A alleles (**Fig. 2e**,**f** and **Supplementary Fig. 4**).

We also found that *Dmp1-Cre* was expressed in tissues other than bone (**Supplementary Fig. 5**). This observation led us to test whether

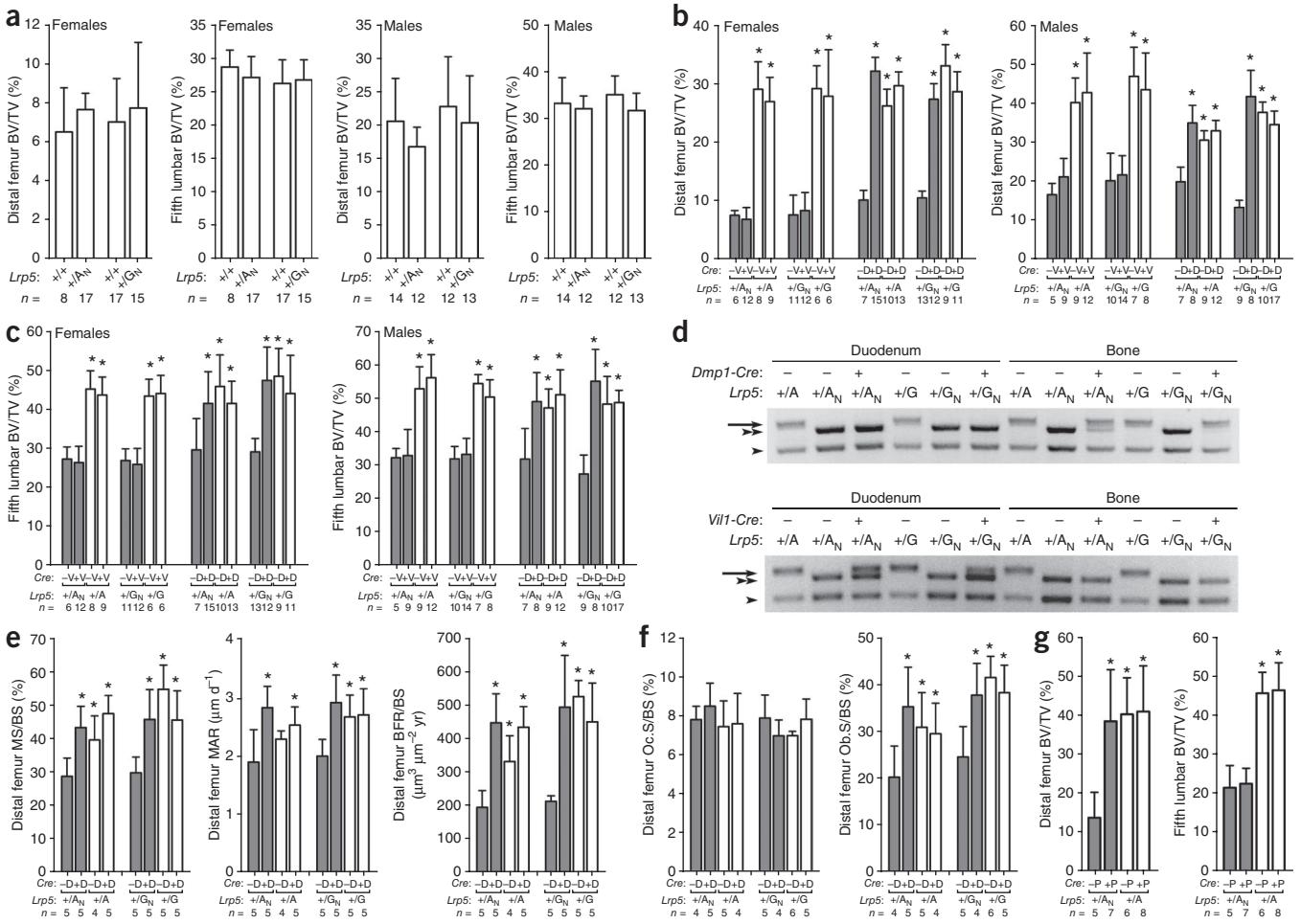

Figure 2 Effect of activating *Lrp5* Neo^R-containing HBM alleles. (**a**) Graphs depicting femoral and vertebral trabecular BV/TV in WT mice and in mice with *Lrp5* Neo^R-containing HBM alleles. (**b**,**c**) Graphs depicting femoral trabecular BV/TV (**b**) and vertebral trabecular BV/TV (**c**) in mice with (shaded bars) and without (unshaded bars) inherited Neo^R-containing *Lrp5* HBM alleles ($+/A_N$ or $+/G_N$, and +/A or +/G, respectively), and with and without *Vil1-Cre* (+V and –V, respectively) or *Dmp1-Cre* (+D and –D, respectively) transgenes. (**d**) Photographs of agarose gels containing PCR amplimers derived from mouse genomic DNA extracted from either duodenum or femur cortex of mice with different *Lrp5* and Cre-transgene genotypes. PCR amplimers correspond to the sizes depicted in **Figure 1a**. Top, amplimers from the *Dmp1-Cre* cross. Bottom, amplimers from the *Vil1-Cre* cross. WT allele (arrowheads), A_N or G_N allele (double arrowheads) A or G allele (arrows). (**e**) Graphs depicting fluorochrome-derived bone formation parameters in the distal femur from 9-week-old female mice that were administered double calcein labeling. Group notations (*x* axis) follow those described for panel **b**. (**f**) Graphs depicting the proportion of distal femur trabecular bone surface covered by osteoclasts (Oc.S; left) and osteoblasts (Ob.S; right). (**g**) Graphs depicting femoral and vertebral trabecular BV/TV in 12-week-old mice with (shaded bars) and without (unshaded bars) inherited Neo^R-containing *Lrp5* HBM alleles ($+/A_N$ and +/A), respectively, and with and without the *Prrx1-Cre* transgene (+P and –P, respectively). MS/BS, MAR, BFR/BS are as defined in **Figure 1**. The numbers of mice studied are indicated. Error bars show means ± s.d. $^*P < 0.05$ versus Neo^R-containing littermates that did not inherit a *Cre* transgene.

Lrp5 signaling outside of bone tissue was responsible for increased bone mass. We began by evaluating the role of Lrp5 in the intestine, as a model has been proposed in which Lrp5 affects bone mass by regulating serotonin (5HT) production in the duodenum[22]. In this model, Lrp5 has no direct role in bone; rather, it affects bone mass accrual by regulating the expression of the enzyme tryptophan hydroxylase 1 (Tph1) in the duodenum[22]. Tph1 is the rate-limiting enzyme for peripheral 5HT synthesis, and the intestine is the principal source of 5HT found in blood[23,24]; another tryptophan hydroxylase (Tph2) produces 5HT in the central nervous system[24–26]. We crossed mice with G/G_N or A/A_N genotypes to mice hemizygous for a transgene, *Vil1-Cre*, that uses a villin 1 (encoded by *Vil1*) regulatory sequence to drive Cre expression in intestinal stem cells[27], from which 5HT-producing enterochromaffin cells are derived. We found that conversion of alleles G_N or A_N to alleles G or A, respectively, in the intestine had no effect on bone mass (**Fig. 2b**,**c** and **Supplementary Fig. 3**). In addition, we found that *Vil1-Cre* drove Cre expression in the intestine but not in bone (**Fig. 2d** and **Supplementary Fig. 5**).

Although our *Vil1-Cre* experiments excluded a substantial role for intestinal Lrp5 expression in the endocrine regulation of bone mass, they did not exclude the possibility that Lrp5 could function elsewhere to regulate bone mass indirectly. Therefore, we tested whether Lrp5 acted locally or systemically to affect bone mass by crossing mice with A/A_N genotypes to mice hemizygous for a transgene, *Prrx1-Cre*; this transgene uses a paired-related homeobox 1 (encoded by *Prrx1*) regulatory sequence to drive Cre expression in cells that form bone in the appendicular skeleton but not in the axial skeleton[28] (**Supplementary Fig. 6**). Conversion of A_N to A in cells that form the appendicular but not the axial skeleton increased bone mass in the limb but not in the spine (**Fig. 2g** and **Supplementary Fig. 6**).

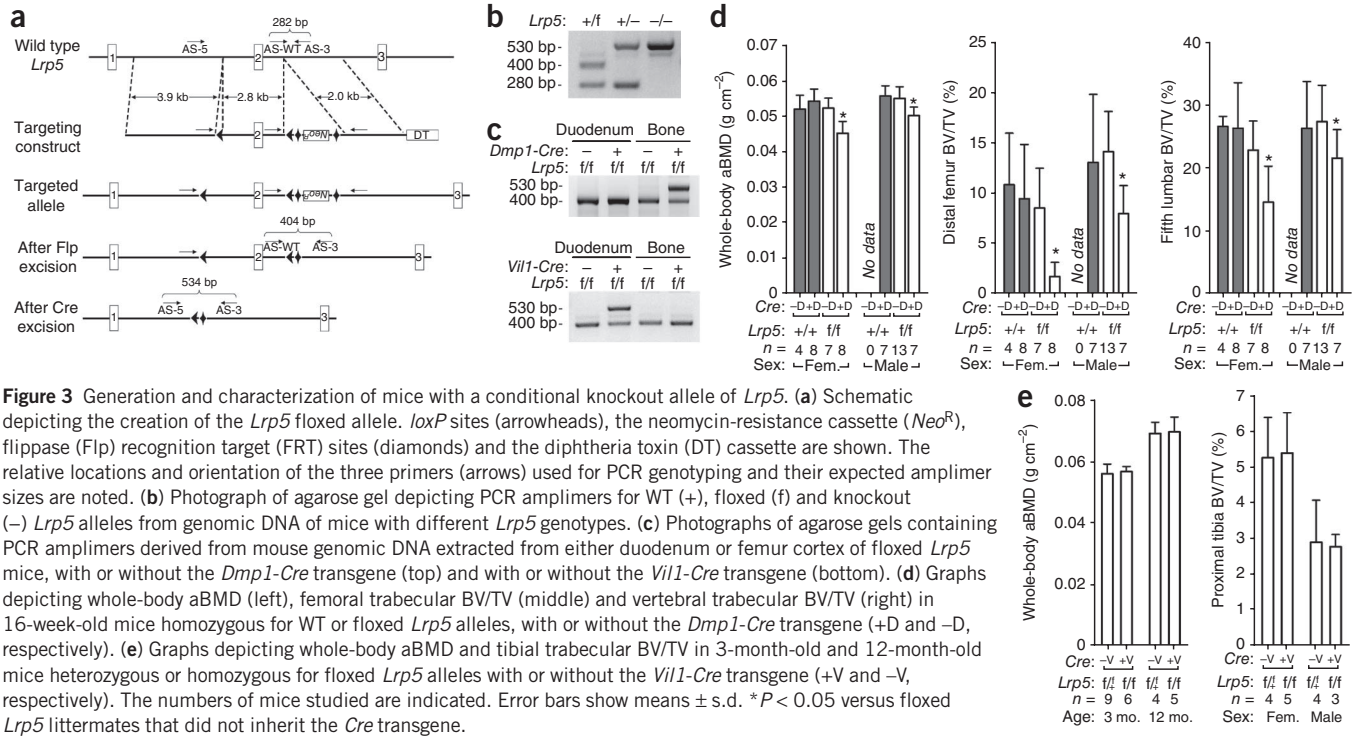

Figure 3 Generation and characterization of mice with a conditional knockout allele of *Lrp5*. (**a**) Schematic depicting the creation of the *Lrp5* floxed allele. *loxP* sites (arrowheads), the neomycin-resistance cassette (Neo^R), flippase (Flp) recognition target (FRT) sites (diamonds) and the diphtheria toxin (DT) cassette are shown. The relative locations and orientation of the three primers (arrows) used for PCR genotyping and their expected amplimer sizes are noted. (**b**) Photograph of agarose gel depicting PCR amplimers for WT (+), floxed (f) and knockout (–) *Lrp5* alleles from genomic DNA of mice with different *Lrp5* genotypes. (**c**) Photographs of agarose gels containing PCR amplimers derived from mouse genomic DNA extracted from either duodenum or femur cortex of floxed *Lrp5* mice, with or without the *Dmp1-Cre* transgene (top) and with or without the *Vil1-Cre* transgene (bottom). (**d**) Graphs depicting whole-body aBMD (left), femoral trabecular BV/TV (middle) and vertebral trabecular BV/TV (right) in 16-week-old mice homozygous for WT or floxed *Lrp5* alleles, with or without the *Dmp1-Cre* transgene (+D and –D, respectively). (**e**) Graphs depicting whole-body aBMD and tibial trabecular BV/TV in 3-month-old and 12-month-old mice heterozygous or homozygous for floxed *Lrp5* alleles with or without the *Vil1-Cre* transgene (+V and –V, respectively). The numbers of mice studied are indicated. Error bars show means ± s.d. $^*P < 0.05$ versus floxed *Lrp5* littermates that did not inherit the *Cre* transgene.

Loss of Lrp5 in osteocytes decreases bone mass

We created a conditional knockout allele of *Lrp5* by flanking exon 2 with *loxP* sites (**Fig. 3a**). Deletion of this exon by Cre-mediated recombination resulted in the production of an *Lrp5* transcript that was frameshifted and that had a premature termination codon shortly after the signal peptide (data not shown). We developed a PCR assay for *Lrp5* WT, floxed and Cre-excised alleles (**Fig. 3b**). We found that bone mass in homozygous floxed (*Lrp5* f/f) mice was indistinguishable from WT mice (**Fig. 3**). Furthermore, bone mass in mice homozygous for Cre-excised alleles was low, similar to other lines of *Lrp5*-knockout mice[10,29] (data not shown). We inactivated *Lrp5* in osteocytes by crossing *Lrp5* f/f mice to *Lrp5* f/f mice that were also hemizygous for *Dmp1-Cre*. We confirmed that *Dmp1-Cre* expression inactivated *Lrp5* in bone and not in

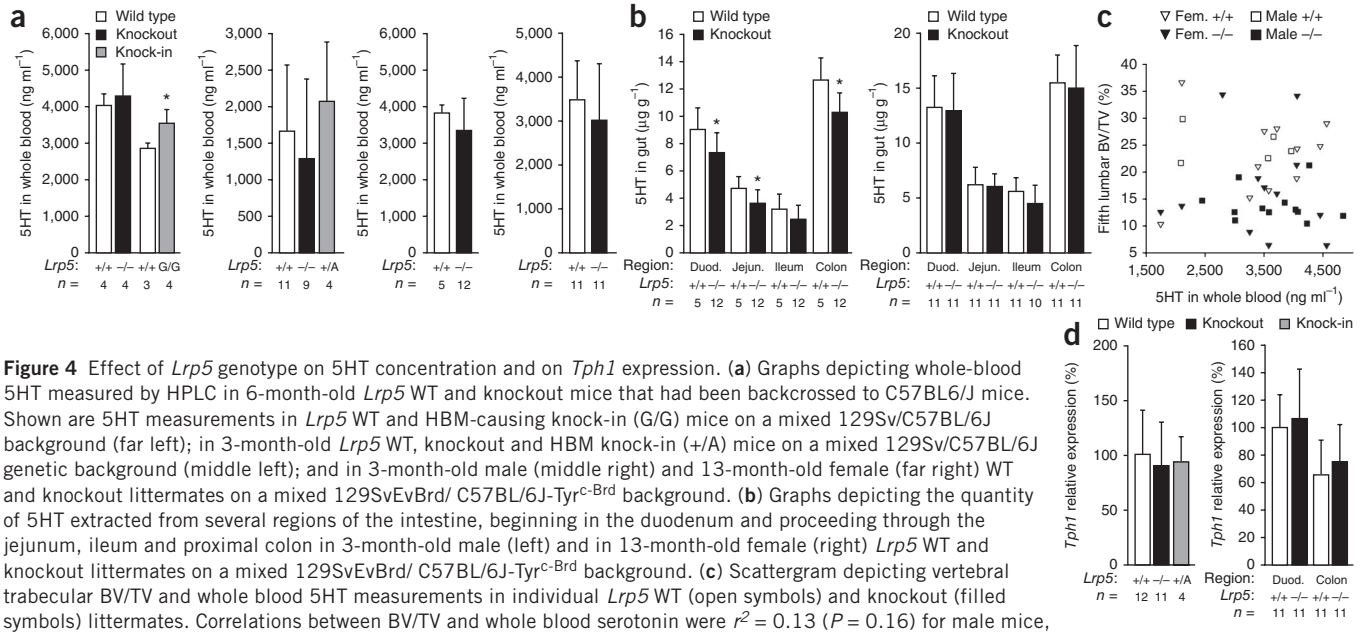

Figure 4 Effect of *Lrp5* genotype on 5HT concentration and on *Tph1* expression. (**a**) Graphs depicting whole-blood 5HT measured by HPLC in 6-month-old *Lrp5* WT and knockout mice that had been backcrossed to C57BL6/J mice. Shown are 5HT measurements in *Lrp5* WT and HBM-causing knock-in (G/G) mice on a mixed 129Sv/C57BL/6J background (far left); in 3-month-old *Lrp5* WT, knockout and HBM knock-in (+/A) mice on a mixed 129Sv/C57BL/6J genetic background (middle left); and in 3-month-old male (middle right) and 13-month-old female (far right) WT and knockout littermates on a mixed 129SvEvBrd/ C57BL/6J-$Tyr^{c\text{-}Brd}$ background. (**b**) Graphs depicting the quantity of 5HT extracted from several regions of the intestine, beginning in the duodenum and proceeding through the jejunum, ileum and proximal colon in 3-month-old male (left) and in 13-month-old female (right) *Lrp5* WT and knockout littermates on a mixed 129SvEvBrd/ C57BL/6J-$Tyr^{c\text{-}Brd}$ background. (**c**) Scattergram depicting vertebral trabecular BV/TV and whole blood 5HT measurements in individual *Lrp5* WT (open symbols) and knockout (filled symbols) littermates. Correlations between BV/TV and whole blood serotonin were $r^2 = 0.13$ ($P = 0.16$) for male mice, and $r^2 = 0.02$ ($P = 0.53$) for female mice. (**d**) Graphs depicting normalized *Tph1* transcript levels in duodenum RNA extracts from *Lrp5* WT, knockout, and HBM-causing knock-in (+/A) mice on a mixed 129Sv/C57BL/6J genetic background (left) and duodenum and colon RNA extracts from *Lrp5* WT and knockout mice on a 129SvEvBrd/ C57BL/6J-$Tyr^{c\text{-}Brd}$ background (right) with *Gapdh* serving as the internal control. The mean *Tph1* expression level for *Lrp5* WT duodenum is set as 100%. The numbers of mice studied are indicated. Error bars show means ± s.d. $^*P < 0.05$ versus WT mice.

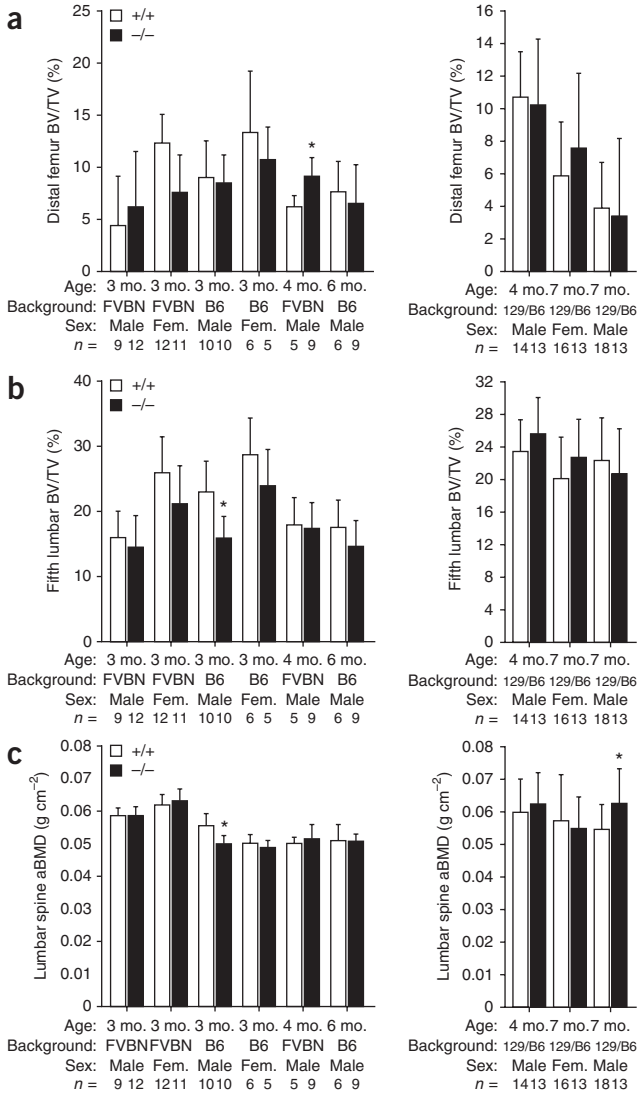

Figure 5 Bone mass in WT and *Tph1*$^{-/-}$ mice. (**a**) Graphs depicting femoral trabecular BV/TV in WT and *Tph1*$^{-/-}$ mice on either FVB/N or C57BL/6 backgrounds (left) or on a mixed 129SvEvBrd/C57BL/6J-Tyr$^{c\text{-}Brd}$ background (right). (**b**) Graphs depicting the vertebral trabecular BV/TV of the fifth lumbar vertebrae in the same mice described in panel **a**. (**c**) Graphs depicting lumbar spine aBMD, as measured by DEXA, in the same mice described in panel **a**. The numbers of mice studied are indicated. Error bars show means ± s.d. *$P < 0.05$ versus WT mice using an unpaired *t* test; none of these differences remain significant after correcting for multiple testing.

duodenum (**Fig. 3c**). Compared to their littermates, mice lacking Lrp5 activity in osteocytes had reduced bone mass (**Fig. 3d** and **Supplementary Fig. 5**). We tested whether inactivation of Lrp5 in the intestine would decrease bone mass by crossing *Lrp5* f/f mice to *Lrp5* f/f mice that were also hemizygous for *Vil1-Cre*; we observed no significant effect on bone mass (**Fig. 3e** and **Supplementary Fig. 5d**).

Lrp5 genotype does not affect intestinal 5HT synthesis

Our data support a mechanism in mice in which Lrp5 functions via the canonical Wnt pathway in osteocytes to regulate bone mass rather than regulating bone mass indirectly via other tissues. However, independent of its role in bone, Lrp5 could also regulate 5HT production in the gut. We measured blood 5HT in mice with different *Lrp5* genotypes, but we saw no association between genotype and the amount of 5HT (**Fig. 4a** and **Supplementary Fig. 7**). We also measured 5HT content in different regions of the intestine in *Lrp5* WT and knockout mice and found only a small decrease in knockout mice (**Fig. 4b**); this is contrary to what would be predicted if the lack of Lrp5 increased *Tph1* expression[22]. We also did not observe a correlation between whole blood 5HT content and bone mass in individual mice (**Fig. 4c**). Finally, with real-time PCR we quantified the level of *Tph1* transcript in RNA extracted from the duodenums of mice with different *Lrp5* genotypes but detected no differences among them (**Fig. 4d**).

Peripheral 5HT synthesis does not affect bone mass

The model[22] by which LRP5 controls serotonin synthesis and regulates bone mass via an endocrine rather than a Wnt-based local mechanism was unexpected[30]. It suggested that bone health could be improved by pharmacologically inhibiting either intestinal serotonin synthesis or the hormone's action on osteoblasts[31]. In fact, pharmacologic inhibition of Tph1 in the intestine was reported to increase bone mass in ovariectomized mice and rats to the same degree as a US Food and Drug Administration–approved anabolic bone therapy, intermittent parathyroid hormone (teriparatide) treatment[32]. Because 5HT in whole blood is nearly absent in *Tph1*$^{-/-}$ mice[23,24], we measured bone mass in *Tph1*$^{-/-}$ and WT mice. After correcting for multiple testing, there were no significant differences in bone mass between *Tph1*$^{-/-}$ and WT mice (**Fig. 5** and **Supplementary Table 3**).

It is possible that *Tph1*$^{-/-}$ mice activate compensatory pathways that keep bone mass at WT levels. This could explain why an increase in bone mass was reported when *Tph1* was conditionally inactivated only in the intestine[22], or when a small molecule was used to inhibit Tph1 in the intestine[32]. Therefore, we treated sham-operated and ovariectomized mice and rats for 6 weeks with a small-molecule Tph1 inhibitor, LP-923941, which is the active enantiomer of a compound, LP-533401 (**Supplementary Table 4**), that has been previously reported to increase bone mass[32]. We selected the LP-923941 dose of 250 mg per kg per day used in our pharmacology studies from a preliminary 7-d dose-response study in mice (**Fig. 6a**).

We found that treating sham-operated and ovariectomized mice with LP-923941 for 6 weeks reduced 5HT content in whole blood by 42% at 2 weeks (2715 versus 4813 ng ml^{-1}, $P < 0.001$) and 44% at 6 weeks (2543 versus 4359 ng ml^{-1}, $P < 0.001$) without influencing brain 5HT content (0.49 versus 0.50 μg g^{-1}) or turnover, as indicated by 5-hydroxyindoleacetic acid levels (0.231 versus 0.229 μg g^{-1}). The ability of LP-923941 to reduce 5HT synthesis in all segments of the intestine was not influenced by ovariectomy ($P < 0.001$, **Fig. 6b**) and was similar in the 7-d dose-response and 6-week pharmacology studies. Reductions in whole blood content and intestinal serotonin content did not influence the amount of serum procollagen 1 N-terminal peptide (P1NP) (a marker of bone formation), trabecular bone mass or cortical bone mass in either sham-operated or ovariectomized mice (**Fig. 6c** and **Supplementary Fig. 8**). In contrast, we found that teriparatide increased bone formation and bone mass in sham-operated and ovariectomized mice (**Fig. 6c** and **Supplementary Fig. 8**).

We also treated sham-operated and ovariectomized rats for 6 weeks with LP-923941, which resulted in a reduction of intestinal 5HT content by 51% and 46%, respectively, compared to vehicle-treated controls (**Fig. 6d**). The reduction in intestinal 5HT content was not accompanied by any change in trabecular or cortical bone mass of the femur, nor did it result in any changes in trabecular bone mass

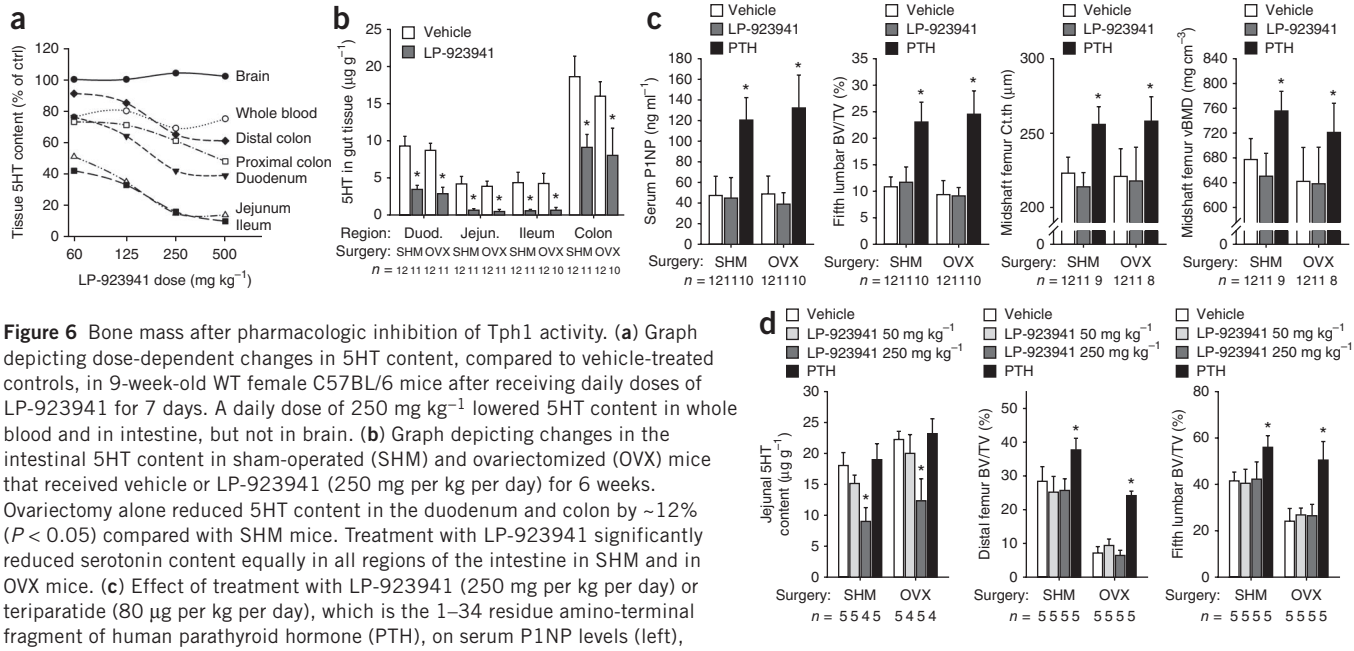

Figure 6 Bone mass after pharmacologic inhibition of Tph1 activity. (**a**) Graph depicting dose-dependent changes in 5HT content, compared to vehicle-treated controls, in 9-week-old WT female C57BL/6 mice after receiving daily doses of LP-923941 for 7 days. A daily dose of 250 mg kg^{-1} lowered 5HT content in whole blood and in intestine, but not in brain. (**b**) Graph depicting changes in the intestinal 5HT content in sham-operated (SHM) and ovariectomized (OVX) mice that received vehicle or LP-923941 (250 mg per kg per day) for 6 weeks. Ovariectomy alone reduced 5HT content in the duodenum and colon by ~12% ($P < 0.05$) compared with SHM mice. Treatment with LP-923941 significantly reduced serotonin content equally in all regions of the intestine in SHM and in OVX mice. (**c**) Effect of treatment with LP-923941 (250 mg per kg per day) or teriparatide (80 µg per kg per day), which is the 1–34 residue amino-terminal fragment of human parathyroid hormone (PTH), on serum P1NP levels (left), vertebral trabecular BV/TV (middle left), midshaft femur cortical thickness (Ct.th; middle right) and midshaft femoral volumetric BMD (right) in SHM and in OVX mice. (**d**) Effect of treating SHM and OVX rats with LP-923941 (50 or 250 mg per kg per day) or teriparatide (80 µg per kg per day) for 6 weeks on jejunal 5HT content (left), femoral trabecular BV/TV (middle) and vertebral trabecular BV/TV (right). The numbers of mice studied are indicated. Error bars show means ± s.d. *$P < 0.05$ versus vehicle-treated mice.

of the fifth lumbar vertebra (**Fig. 6d**). However, daily injections with teriparatide significantly increased bone mass in both the femur and the vertebral body of sham-operated and ovariectomized rats (**Fig. 6d** and **Supplementary Fig. 9**).

DISCUSSION

Our *in vivo* data indicate that Lrp5 acts in osteocytes and perhaps in some late-stage osteoblasts to effect changes in bone mass via canonical Wnt signaling. *Axin2*, a downstream target of Wnt signaling, is more highly expressed in bone from mice with HBM-causing alleles, as is a *lacZ* reporter of canonical Wnt signaling (**Supplementary Fig. 1**). These results are consistent with *in vitro* studies of LRP5-mediated Wnt signaling, which reported that HBM mutations cause LRP5 to be less inhibited by the endogenous inhibitors DKK1 and SOST than WT LRP5[9,11,33,34]. DKK1 is expressed by many cells, including osteocytes, and a complete lack of *Dkk1* is embryonic lethal; however, mice with partial loss-of-function mutations in *Dkk1* have increased bone mass, which is consistent with this protein acting as a negative regulator of bone formation[16,35]. SOST is principally expressed by mature osteocytes, and when it is genetically absent in humans and in mice it causes a phenotype that is similar to the phenotype resulting from HBM-causing mutations in *LRP5*[4,5,15]. The strong expression of SOST by mature bone cells suggests that it functions as a tonic negative regulator of new bone formation (**Supplementary Fig. 10**). In mice, the mechanical loading of bone, which is a potent inducer of new bone formation *in vivo*, reduces Sost expression by osteocytes[36] and increases the expression of Wnt target genes[37,38]. Therefore, by being less sensitive to endogenous inhibitors, Lrp5 HBM mutants are likely to induce new bone formation in the absence of mechanical load or at lower mechanical load (**Supplementary Fig. 10**). Conversely, mice that lack Lrp5 have a blunted anabolic response to mechanical load[39], which is consistent with insufficient Wnt signaling in $Lrp5^{-/-}$ osteocytes (**Supplementary Fig. 10**).

Lrp5 is also expressed during osteoblast commitment and differentiation[1,40]. Therefore, similarly to other signaling pathways that influence cellular differentiation at several stages[41,42], Lrp5 signaling may influence other aspects of osteoblast differentiation. This speculation is compatible with studies noting that, in the absence of canonical Wnt signaling, differentiating mesenchymal stem cells adopt chondrogenic and adipogenic fates instead of osteoblastic fates[43–46]. However, these studies blocked canonical Wnt signaling by conditionally inactivating β-catenin. LRP5 and its closest-related mammalian paralog, LRP6, are both able to transduce Wnt signaling *in vitro*, and they have overlapping and nonredundant roles *in vivo* during gastrulation and skeletal patterning[10,47]. Therefore, LRP6 may be able to compensate for LRP5 during some stages of osteoblast differentiation.

We found that inducing the *Lrp5* HBM allele in osteocytes had the same effect on bone mass as was observed when the active *Lrp5* HBM allele was inherited. Conversely, *Dmp1-Cre*-mediated inactivation of *Lrp5* in osteocytes caused a decrease in bone mass compared to WT mice. Taken together, these data indicate that Lrp5 signaling by mature bone cells regulates bone mass and, in the case of the HBM-causing mutation, is sufficient to recapitulate the inherited HBM phenotype. Further support for this conclusion derives from studies in which we caused the *Lrp5* HBM allele to become active in cells that contribute to the appendicular skeleton but not to the axial skeleton. Bone mass increased only at skeletal sites where the HBM-associated allele was active.

Our results do not support a model in which Lrp5 regulates bone mass via the regulation of peripheral 5HT synthesis in the duodenum[22]. When we activated *Lrp5* HBM or inactivated WT *Lrp5* in 5HT-producing enterochromaffin cells, we found no effect on bone mass. In addition, we found no *Lrp5* genotype-specific differences in the amount of whole blood 5HT, nor did we observe any effect on bone mass after genetically or pharmacologically lowering peripheral 5HT production.

Currently, we do not know the origin of the difference in the results of our study and those of prior studies[22,32]. Perhaps differences in the design of the *Lrp5* conditional alleles, the transgenic mice that were used to produce cell type–specific Cre recombination within bone and intestine, the assays used to measure 5HT, the use of conditional versus global *Tph1* knockout alleles, the vivariums in which the mice were raised or the trial design for pharmacologic inhibition of Tph1 in ovariectomized mice and rats account for the differing results (also see **Supplementary Methods**).

We created mice with knock-in HBM-causing alleles in which the gene's intron-exon structure remained intact. An earlier study inserted an HBM-causing *Lrp5* cDNA with a C-terminal Flag tag into the first exon of *Lrp5*[22]. We used a *Dmp1-Cre* transgene that is expressed in osteocytes and in some late-stage osteoblasts, whereas the other study[22] used a *Col1a1-Cre* transgene (with a 2.3-kb collagen, type 1, α-1 promoter to drive Cre expression) that is expressed earlier in the process of osteoblastic differentiation[48]. We used a different *Vil1-Cre* transgenic mouse line than the earlier study[22], although both lines expressed Cre in intestinal stem cells. Nevertheless, it remains possible that inefficient Cre-mediated recombination or off-target sites of Cre expression account for some of the divergent results between our study and the other study[22].

We found no association between *Lrp5* genotype and serum 5HT concentration. However, the concentration of 5HT in serum depends on the efficiency of 5HT release from platelets during clot formation, which, in turn, is affected by the collection and clotting method as well as the clotting time[49]. As such, serum measures can be unreliable within and across studies. In contrast, as long as the capacity of platelets to store 5HT is not exceeded, whole blood 5HT content correlates well with free circulating 5HT concentration[50]. Therefore, we also measured whole blood 5HT by HPLC[23]. The amount of 5HT in whole blood did not correlate with *Lrp5* genotype or with bone mass. Because the amount of whole blood 5HT can be influenced by other factors, such as inflammation and infection, it is possible that environmental differences between the present study and the earlier study[22] account for the divergent 5HT results.

We studied bone mass in $Tph1^{-/-}$ mice, whereas *Tph1* was inactivated using *Vil1-Cre* in the previous study[22]. $Tph1^{-/-}$ mice may have activated compensatory pathways to normalize bone mass, whereas mice with conditional *Tph1* inactivation may not. We tested this possibility by pharmacologically inhibiting 5HT synthesis in the intestine. We used the active enantiomer of a small-molecule inhibitor previously reported to affect bone mass[32]. We studied mice that had undergone ovariectomy a year before receiving the pharmacologic agent and found no effect on bone mass compared to vehicle-treated controls (**Fig. 6**); in contrast, teriparatide had a strong anabolic effect. We examined aged ovariectomized mice, because women in their first decade after menopause are a major target population for anabolic osteoporosis therapy. However, our ovariectomy model differed from that used in the earlier study in which mice had undergone ovariectomy less than 2 months before receiving the pharmacologic agent[32]. Therefore, we used a rat model in which we began pharmacologic Tph1 inhibition 5 weeks after ovariectomy; this is within the time frame used in the previous study[32]. Again, we observed no effect of Tph1 inhibition on bone mass compared to vehicle-treated controls, whereas teriparatide had a robust bone anabolic effect (**Fig. 6**). However, because we only studied the active enantiomer, we cannot exclude the possibility that the inactive enantiomer increases bone mass via a mechanism that is independent of Tph1 inhibition.

Although *Lrp5* genotype may affect peripheral serotonin synthesis in some contexts[22], in the present study we did not observe Lrp5-mediated effects on peripheral 5HT abundance or Tph1-mediated effects on bone mass. Therefore we think it unlikely that the mechanism by which LRP5 normally affects human bone mass involves intestinal 5HT synthesis. Instead, our data suggest that LRP5 functions in bone to control bone mass, and they are consistent with the notion that the receptor participates in the adaptive response of bone to mechanical load (Wolff's law)[51]. Therapies aimed at enhancing these functions of LRP5 in humans may benefit individuals who have skeletal fragility as a result of low bone mass.

METHODS

Methods and any associated references are available in the online version of the paper at http://www.nature.com/naturemedicine/.

Note: Supplementary information is available on the Nature Medicine website.

ACKNOWLEDGMENTS

We thank members of our laboratories for technical support: B. Newby, K. Kurek and E. Boyden for assistance with the HBM mouse studies; G. Zhou for assistance with histomorphometry; M. Niedecker and E. Kleinschmidt for assistance with radiography; the Case Transgenic and Targeting Facility; K. Sisson and P. Swiatek of the Van Andel Research Institute Mouse Germline Modification Core; B. Eagleson and the staff of the Van Andel Research Institute Vivarium; J. Bardenhagen, J. Greer, S. Jeter-Jones, J. Liu, M.K. Shadoan, D.D. Smith, W. Xiong and A. Yu of Lexicon Pharmaceuticals; and F. Bourgondien, R. Zhang and S. Yeh of Merck Sharp & Dohme Research Laboratories. This work was supported by the following grants: US National Institutes of Health (NIH) grant AR53237 (to A.G.R.); Public Health Service Career Development Award (UL 1RR025761-02) (to P.J.N.); NIH grant (GM74241) and a Leukemia and Lymphoma Society Scholarship (both to X.H.); NIH grant AR053293 and Van Andel Research Institute funds (to B.O.W.). M.L.W. is an investigator with the Howard Hughes Medical Institute.

AUTHOR CONTRIBUTIONS

Y.C. created and did studies on the mice with the *Lrp5* HBM alleles and measured serum serotonin levels by competitive ELISA. P.J.N. did radiographic imaging and biomechanical testing on the mice with HBM-associated alleles. B.T.M. contributed to the serotonin and *Tph1* qRT-PCR measurements in HBM-causing and *Lrp5* knockout mice. C.R.Z. did multiple studies using the conditional *Lrp5* knockout mice. N.A. studied the $Tph1^{-/-}$ mice, and with S.M. measured whole blood serotonin levels from HBM-causing and *Lrp5*-knockout mice by HPLC. D.R.R. generated the conditional *Lrp5* knockout strain and Z.Z. participated in conditional inactivation of this allele using different Cre transgenes. C.M.J. carried out the *Prrx1-Cre* experiments. R.B., F.M. and Q.M.Y. organized studies on *Lrp5*- and *Tph* -knockout mice, and also organized the mouse pharmacology experiment. H.G. and J.A.G. organized the rat pharmacology experiment. R.A.C., X.H., M.B., D.R.P., Q.L., B.Z., B.O.W., A.G.R. and M.L.W. designed experiments and provided reagents and financial support. M.L.W. prepared the first draft of the manuscript. All co-authors contributed detailed methods and results, and revised and approved the manuscript.

COMPETING FINANCIAL INTERESTS

The authors declare competing financial interests: details accompany the full-text HTML version of the paper at http://www.nature.com/naturemedicine/.

Published online at http://www.nature.com/naturemedicine/.
Reprints and permissions information is available online at http://www.nature.com/reprints/index.html.

1. Gong, Y. *et al.* LDL receptor-related protein 5 (LRP5) affects bone accrual and eye development. *Cell* **107**, 513–523 (2001).
2. Little, R.D. *et al.* A mutation in the LDL receptor-related protein 5 gene results in the autosomal dominant high-bone-mass trait. *Am. J. Hum. Genet.* **70**, 11–19 (2002).
3. Boyden, L.M. *et al.* High bone density due to a mutation in LDL-receptor-related protein 5. *N. Engl. J. Med.* **346**, 1513–1521 (2002).
4. Balemans, W. *et al.* Increased bone density in sclerosteosis is due to the deficiency of a novel secreted protein (SOST). *Hum. Mol. Genet.* **10**, 537–543 (2001).
5. Brunkow, M.E. *et al.* Bone dysplasia sclerosteosis results from loss of the SOST gene product, a novel cystine knot-containing protein. *Am. J. Hum. Genet.* **68**, 577–589 (2001).

6. Morello, R. *et al.* CRTAP is required for prolyl 3-hydroxylation and mutations cause recessive osteogenesis imperfecta. *Cell* **127**, 291–304 (2006).
7. Ai, M., Heeger, S., Bartels, C.F. & Schelling, D.K. Clinical and molecular findings in osteoporosis-pseudoglioma syndrome. *Am. J. Hum. Genet.* **77**, 741–753 (2005).
8. Van Wesenbeeck, L. *et al.* Six novel missense mutations in the LDL receptor-related protein 5 (LRP5) gene in different conditions with an increased bone density. *Am. J. Hum. Genet.* **72**, 763–771 (2003).
9. Ai, M., Holmen, S.L., Van Hul, W., Williams, B.O. & Warman, M.L. Reduced affinity to and inhibition by DKK1 form a common mechanism by which high bone mass-associated missense mutations in LRP5 affect canonical Wnt signaling. *Mol. Cell. Biol.* **25**, 4946–4955 (2005).
10. Holmen, S.L. *et al.* Decreased BMD and limb deformities in mice carrying mutations in both Lrp5 and Lrp6. *J. Bone Miner. Res.* **19**, 2033–2040 (2004).
11. Semenov, M.V. & He, X. LRP5 mutations linked to high bone mass diseases cause reduced LRP5 binding and inhibition by SOST. *J. Biol. Chem.* **281**, 38276–38284 (2006).
12. Kato, M. *et al.* Cbfa1-independent decrease in osteoblast proliferation, osteopenia, and persistent embryonic eye vascularization in mice deficient in Lrp5, a Wnt coreceptor. *J. Cell Biol.* **157**, 303–314 (2002).
13. Kokubu, C. *et al.* Skeletal defects in ringelschwanz mutant mice reveal that Lrp6 is required for proper somitogenesis and osteogenesis. *Development* **131**, 5469–5480 (2004).
14. Nakanishi, R. *et al.* Secreted frizzled-related protein 4 is a negative regulator of peak BMD in SAMP6 mice. *J. Bone Miner. Res.* **21**, 1713–1721 (2006).
15. Li, X. *et al.* Targeted deletion of the sclerostin gene in mice results in increased bone formation and bone strength. *J. Bone Miner. Res.* **23**, 860–869 (2008).
16. Morvan, F. *et al.* Deletion of a single allele of the *Dkk1* gene leads to an increase in bone formation and bone mass. *J. Bone Miner. Res.* **21**, 934–945 (2006).
17. Babij, P. *et al.* High bone mass in mice expressing a mutant LRP5 gene. *J. Bone Miner. Res.* **18**, 960–974 (2003).
18. Zhang, Y. *et al.* The LRP5 high-bone-mass G171V mutation disrupts LRP5 interaction with Mesd. *Mol. Cell. Biol.* **24**, 4677–4684 (2004).
19. Maretto, S. *et al.* Mapping Wnt/β-catenin signaling during mouse development and in colorectal tumors. *Proc. Natl. Acad. Sci. USA* **100**, 3299–3304 (2003).
20. Jho, E.H. *et al.* Wnt/β-catenin/Tcf signaling induces the transcription of Axin2, a negative regulator of the signaling pathway. *Mol. Cell. Biol.* **22**, 1172–1183 (2002).
21. Lu, Y. *et al.* DMP1-targeted Cre expression in odontoblasts and osteocytes. *J. Dent. Res.* **86**, 320–325 (2007).
22. Yadav, V.K. *et al.* Lrp5 controls bone formation by inhibiting serotonin synthesis in the duodenum. *Cell* **135**, 825–837 (2008).
23. Liu, Q. *et al.* Discovery and characterization of novel tryptophan hydroxylase inhibitors that selectively inhibit serotonin synthesis in the gastrointestinal tract. *J. Pharmacol. Exp. Ther.* **325**, 47–55 (2008).
24. Walther, D.J. *et al.* Synthesis of serotonin by a second tryptophan hydroxylase isoform. *Science* **299**, 76 (2003).
25. Alenina, N. *et al.* Growth retardation and altered autonomic control in mice lacking brain serotonin. *Proc. Natl. Acad. Sci. USA* **106**, 10332–10337 (2009).
26. Savelieva, K.V. *et al.* Genetic disruption of both tryptophan hydroxylase genes dramatically reduces serotonin and affects behavior in models sensitive to antidepressants. *PLoS ONE* **3**, e3301 (2008).
27. Madison, B.B. *et al.* Cis elements of the villin gene control expression in restricted domains of the vertical (crypt) and horizontal (duodenum, cecum) axes of the intestine. *J. Biol. Chem.* **277**, 33275–33283 (2002).
28. Logan, M. *et al.* Expression of Cre recombinase in the developing mouse limb bud driven by a Prxl enhancer. *Genesis* **33**, 77–80 (2002).
29. Iwaniec, U.T. *et al.* PTH stimulates bone formation in mice deficient in Lrp5. *J. Bone Miner. Res.* **22**, 394–402 (2007).
30. Long, F. When the gut talks to bone. *Cell* **135**, 795–796 (2008).
31. Rosen, C.J. Serotonin rising—the bone, brain, bowel connection. *N. Engl. J. Med.* **360**, 957–959 (2009).
32. Yadav, V.K. *et al.* Pharmacological inhibition of gut-derived serotonin synthesis is a potential bone anabolic treatment for osteoporosis. *Nat. Med.* **16**, 308–312 (2010).
33. Balemans, W. *et al.* The binding between sclerostin and LRP5 is altered by DKK1 and by high-bone mass LRP5 mutations. *Calcif. Tissue Int.* **82**, 445–453 (2008).
34. Ellies, D.L. *et al.* Bone density ligand, Sclerostin, directly interacts with LRP5 but not LRP5G171V to modulate Wnt activity. *J. Bone Miner. Res.* **21**, 1738–1749 (2006).
35. MacDonald, B.T. *et al.* Bone mass is inversely proportional to Dkk1 levels in mice. *Bone* **41**, 331–339 (2007).
36. Robling, A.G. *et al.* Mechanical stimulation of bone in vivo reduces osteocyte expression of Sost/sclerostin. *J. Biol. Chem.* **283**, 5866–5875 (2008).
37. Bonewald, L.F. & Johnson, M.L. Osteocytes, mechanosensing and Wnt signaling. *Bone* **42**, 606–615 (2008).
38. Robinson, J.A. *et al.* Wnt/β-catenin signaling is a normal physiological response to mechanical loading in bone. *J. Biol. Chem.* **281**, 31720–31728 (2006).
39. Sawakami, K. *et al.* The Wnt co-receptor LRP5 is essential for skeletal mechanotransduction but not for the anabolic bone response to parathyroid hormone treatment. *J. Biol. Chem.* **281**, 23698–23711 (2006).
40. Dong, Y. *et al.* Molecular cloning and characterization of LR3, a novel LDL receptor family protein with mitogenic activity. *Biochem. Biophys. Res. Commun.* **251**, 784–790 (1998).
41. Fuccillo, M., Joyner, A.L. & Fishell, G. Morphogen to mitogen: the multiple roles of hedgehog signalling in vertebrate neural development. *Nat. Rev. Neurosci.* **7**, 772–783 (2006).
42. Zhong, W. & Chia, W. Neurogenesis and asymmetric cell division. *Curr. Opin. Neurobiol.* **18**, 4–11 (2008).
43. Day, T.F., Guo, X., Garrett-Beal, L. & Yang, Y. Wnt/β-catenin signaling in mesenchymal progenitors controls osteoblast and chondrocyte differentiation during vertebrate skeletogenesis. *Dev. Cell* **8**, 739–750 (2005).
44. Hill, T.P., Spater, D., Taketo, M.M., Birchmeier, W. & Hartmann, C. Canonical Wnt/β-catenin signaling prevents osteoblasts from differentiating into chondrocytes. *Dev. Cell* **8**, 727–738 (2005).
45. Hu, H. *et al.* Sequential roles of Hedgehog and Wnt signaling in osteoblast development. *Development* **132**, 49–60 (2005).
46. Kang, S. *et al.* Wnt signaling stimulates osteoblastogenesis of mesenchymal precursors by suppressing CCAAT/enhancer-binding protein alpha and peroxisome proliferator-activated receptor gamma. *J. Biol. Chem.* **282**, 14515–14524 (2007).
47. Kelly, O.G., Pinson, K.I. & Skarnes, W.C. The Wnt co-receptors Lrp5 and Lrp6 are essential for gastrulation in mice. *Development* **131**, 2803–2815 (2004).
48. Dacquin, R., Starbuck, M., Schinke, T. & Karsenty, G. Mouse alpha1(I)-collagen promoter is the best known promoter to drive efficient Cre recombinase expression in osteoblast. *Dev. Dyn.* **224**, 245–251 (2002).
49. Ingebretsen, O.C., Bakken, A.M. & Farstad, M. Liquid chromatography of serotonin and adenine nucleotides in blood platelets, illustrated by evaluation of functional integrity of platelet preparations. *Clin. Chem.* **31**, 695–698 (1985).
50. Anderson, G.M., Stevenson, J.M. & Cohen, D.J. Steady-state model for plasma free and platelet serotonin in man. *Life Sci.* **41**, 1777–1785 (1987).
51. Wolff, J. *The Law of Bone Remodeling* (Springer-Verlag, 1892).

ONLINE METHODS

Generation of new genetically modified mouse strains. We created conditional *Lrp5* HBM-causing and knockout alleles by homologous recombination in ES cells (see **Supplementary Methods**). We used targeting vectors containing different missense mutations (p.G171V or p.A214V) for the HBM-causing knock-in mice. We included a floxed neomycin-resistance cassette (Neo^R) for selection (**Fig. 1a**). We bred knock-in mice that retained Neo^R and mice in which Neo^R had been Cre-excised. We created a floxed knockout allele by placing flanking *loxP* sites in the same orientation around exon 2. We included a flippase recognition target–flanked neomycin-resistance cassette that we subsequently excised (**Fig. 3a**). We bred mice that retained the floxed exon 2 and mice in which exon 2 had been Cre-excised. Genotyping was done by PCR. Other mice used in these studies have been described previously: *EIIa-Cre* (ref. 52), *FLPer* (ref. 53), *Cmv-Cre* (ref. 54), *Dmp1-Cre* (ref. 21), *Vil1-Cre* (ref. 27), *Prrx1-Cre* (ref. 28), *BAT-lacZ* (ref. 19), $Lrp5^{-/-}$ (refs. 10,29,55), $Tph1^{-/-}$ (refs. 23,24) and $Rosa26^{mTmG}$ (ref. 56). Details and suppliers are included in the **Supplementary Methods**.

Assessment of bone properties. We did quantitative histomorphometry in mice as previously described[39]. We analyzed one 6-µm coronal section from the distal femur of each mouse for mineralizing surface (MS/BS; %), mineral apposition rate (MAR; µm per day) and bone formation rate (BFR; μm^3 per μm^2 per year). We measured three-dimensional morphometric properties in the cortical and trabecular bone of mouse distal femoral metaphyses and fifth lumbar vertebrae by µCT. We did whole-body DEXA to measure aBMD (in gm cm^{-2}) and bone mineral content (in gm) in the postcranial skeleton, in the lumbar spine (L3–L5, inclusive) and in individual bones. We did biomechanical testing on the left femora by loading them to failure in monotonic compression using a crosshead speed of 0.2 mm s^{-1}, during which we collected force and displacement measurements every 0.005 s. From the force versus displacement curves, we calculated ultimate force (in N), yield force (in N), stiffness (in N mm^{-1}) and energy to failure (in mJ). Details are included in the **Supplementary Methods**.

Measurement of serotonin and *Tph1*, *lacZ*, and *Axin2* mRNA expression. We measured whole blood serotonin by two methods[23,57]. For serum serotonin measures, we used blood that was collected from the retro-orbital sinus and clotted at room temperature. We recovered serum by centrifugation at 4 °C, 17,000*g* for 25 min and then assayed serotonin by competitive ELISA (Fitzgerald Industries International). We extracted and measured serotonin from different segments of intestine as previously described[23]. We did quantitative RT-PCR for intestinal *Tph1* expression using total RNA recovered from the duodenum. We did quantitative RT-PCR for *lacZ* and *Axin2* expression using RNA recovered from cortical bone tissue of 8-week-old male and female *BAT-lacZ* transgenic mice with *Lrp5* WT and A/A genotypes. Experimental and reagent details are included in the **Supplementary Methods**.

Pharmacological inhibition of gut Tph1 activity. We treated sham-operated and ovariectomized mice and rats with the Tph1 inhibitor LP-923941 (Lexicon Pharmaceuticals). This compound is the active enantiomer of the Tph1 inhibitor LP-533401 (Lexicon Pharmaceuticals) examined previously[23,32]. Compared with LP-533401, LP-923941 has approximately twice the potency in enzymatic and cell-based assays, with the inactive enantiomer having greatly reduced potency (**Supplementary Table 4**). We treated animals by oral gavage for 6 weeks with 250 mg per kg per day of LP-923941 or with vehicle (10% (vol/vol) propylene glycol) alone. To serve as a positive control for bone formation, we subcutaneously injected sham-operated and ovariectomized mice and rats for 6 weeks with teriparatide (hPTH 1-34; Bachem) at a dose of 80 µg per kg per day or with vehicle (20 mM NaH_2PO_4 in 0.9% (wt/vol) saline) alone. For the P1NP assay, we collected blood in heparinized capillary tubes by retro-orbital bleeding. We measured P1NP using a rat/mouse P1NP enzyme immunoassay (Immunodiagnostic Systems). Additional details and sources of reagents are included in the **Supplementary Methods**.

Statistical analyses. We tested longitudinal data for differences among genotypes using single-classification repeated-measures analysis of variance (ANOVA). We tested cross-sectional data (µCT data, biomechanical properties, serotonin measurements) across genotypes for significant differences using single-classification ANOVA, followed by the Sheffe *post hoc* comparison to probe pairwise comparisons in the event that the omnibus ANOVA was significant. We did statistical calculations in StatView 5.0 (SAS). We did two- or three-factor ANOVAs for the pharmacology studies with SPSS, version 11.5.0 (SPSS). We set the experimentwise error rate at $\alpha = 0.05$ for all tests. Details are included in the **Supplementary Methods**.

Additional methods. Detailed methodology is described in the **Supplementary Methods**.

52. Lakso, M. *et al.* Efficient in vivo manipulation of mouse genomic sequences at the zygote stage. *Proc. Natl. Acad. Sci. USA* **93**, 5860–5865 (1996).
53. Farley, F.W., Soriano, P., Steffen, L.S. & Dymecki, S.M. Widespread recombinase expression using FLPeR (flipper) mice. *Genesis* **28**, 106–110 (2000).
54. Schwenk, F., Baron, U. & Rajewsky, K. A cre-transgenic mouse strain for the ubiquitous deletion of loxP-flanked gene segments including deletion in germ cells. *Nucleic Acids Res.* **23**, 5080–5081 (1995).
55. Clément-Lacroix, P. *et al.* Lrp5-independent activation of Wnt signaling by lithium chloride increases bone formation and bone mass in mice. *Proc. Natl. Acad. Sci. USA* **102**, 17406–17411 (2005).
56. Muzumdar, M.D., Tasic, B., Miyamichi, K., Li, L. & Luo, L. A global double-fluorescent Cre reporter mouse. *Genesis* **45**, 593–605 (2007).
57. Tenner, K., Qadri, F., Bert, B., Voigt, J.P. & Bader, M. The mTPH2 C1473G single nucleotide polymorphism is not responsible for behavioural differences between mouse strains. *Neurosci. Lett.* **431**, 21–25 (2008).